High-fidelity Structural optimization of a tow-steered composite wing

Timothy R. Brooks[1], John T. Hwang [2], Graeme J. Kennedy [3], Joaquim R. R. A. Martins [4]

[1] University of Michigan, Ann Arbor, Michigan, USA, timryanb@umich.edu
[2] University of Michigan, Ann Arbor, Michigan, USA, hwangjt@umich.edu
[3] Georgia Institute of Technology, Atlanta, Georgia, USA, graeme.kennedy@aerospace.gatech.edu
[4] University of Michigan, Ann Arbor, Michigan, USA, jrram@umich.edu

1. Abstract
Composite materials are now making their way into the primary structures of large transport aircraft and have contributed to more efficient airframes. However, the composites used so far consist in conventional plies with fixed angles. The introduction of the capability to manufacture tow-steered composites opens the door to more efficient airframes by enabling more tailored structures. This paper will propose a general method for setting up tow-steered composite structural optimization problems. This method also features a method for mapping potentially thousands of discrete ply angles to a complex structure of interest. This mapping is amenable to adjoint gradient computation, which would otherwise be prohibitively expensive for any problem with a high enough fidelity to be of use. While the motivation of this method is to parameterize and optimize composite tow angles, it can handle both spatially varying tow angle and thickness variables separately and together. Several structural problems are proposed and their results presented. From these results we show that this method offers a robust design parameterization while being general enough to be applicable to a large number of structures. While purely structural, the presented methodology can be extend to aerostructural design optimization.

2. Keywords: Structural optimization, tow-steered composites, composites, fuel burn, flexible wing

3. Introduction
Tow steering is a relatively new composite manufacturing technique in which a machine is used to distribute composite fibers with a continuously varying direction on a surface, as opposed to the typical uni-directional laminae. This effectively gives the designer control over the local stiffness properties of their structures and enables the tailoring of the deflected shape for a prescribed load. This allows the structure to deform in ways that reduce stress concentrations, or result in passive load alleviation. With such unprecedented control over the behavior of the structure, a natural question to ask is: How can we find the optimal fiber distribution to maximize the performance of our structure? This question can be answered with multidisciplinary design optimization (MDO). Examples of these problems would include designing a wing to defect in flight to optimally reduce fuel burn, such as in Kenway and Martins [8], or designing structure that can withstand complex load distributions while minimizing weight. Spatially varying composite ply distribution optimization has been studied by Kennedy and Martins [6] and Hvejsel et al. [1] among others. However in these cases the fiber angles were forced to take discrete values due to manufacturing constraints. In the present paper we now relax that constraint and allow all angles to take continuous values. Continuous tow steered optimization has been investigated by groups such as Jegley et al. [4] and Jutte al.[5]. The difference is the paper proposes a new method for tow parametrization and optimization over a full 3D model using gradient based optimization techniques.

4. Method
In this section, we describe the method for performing tow-steering via numerical optimization. The high-level approach is to use a shell-element structural solver with the shell stiffness computed from the local tow angle through first-order shear deformation theory (FSDT). The shell stiffness matrices are permitted to vary within each element, reusing the element shape functions. The tow angle distribution across a structural component is smoothly parametrized using B-spline surfaces, so the design variables for optimization are the B-spline control points of this parameterization. A necessary intermediate step between the B-spline parameterization and computation of the stiffness matrices is to perform a local tow angle transformation to reverse the effect of each quadrilateral elements orientation because we use unstructured quad meshes, in general. We use a gradient-based optimizer with adjoint-based derivative computation to enable optimization with a large number of design variables. Figure 1 illustrates the steps involved in mapping the design variables to the objective and constraint functions using an extended design structure matrix (XDSM) [9] diagram.

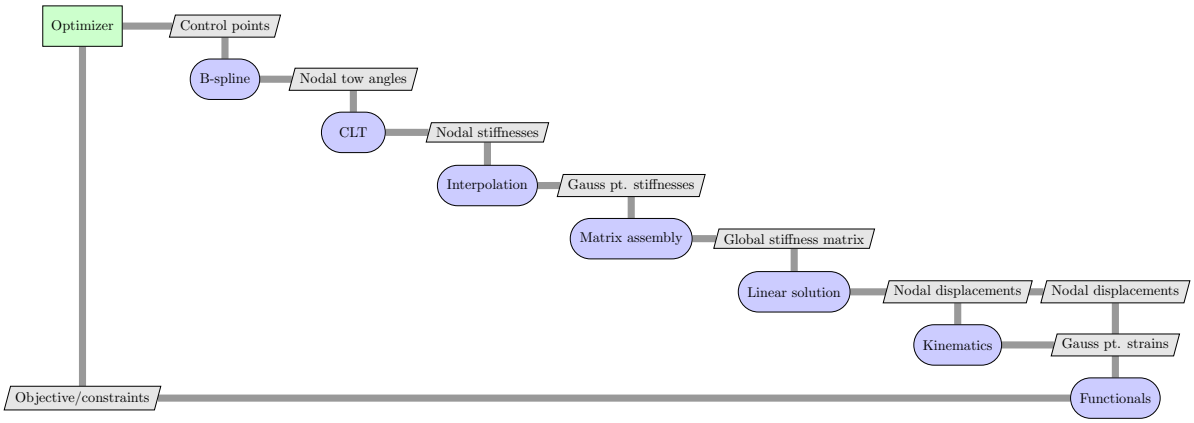

Figure 1: Extended design structure matrix (XDSM) diagram showing the steps in the tow-steering optimization.

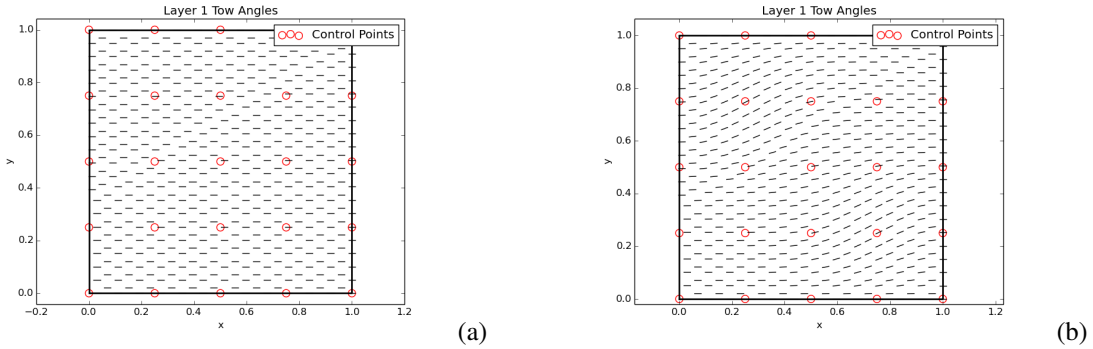

(a) Constant (b) Perturbed

Figure 2: B-spline control points and the resulting tow angle distributions.

Section 4.1 describes the B-spline parameterization and Sec. 4.2 discusses the FSDT formulation and the aforementioned local angle transformation. Section 4.3 provides brief descriptions of the structural solver and optimizer used in this work.

4.1 B-spline parameterization

A unique requirement of the tow-steering problem is a parameterization that ensures that the tow paths on each structural component are smooth, while maintaining freedom for the optimizer. We achieved such a parameterization by using B-spline surfaces to define a continuous and smooth tow angle distribution within each structural component. Additional smoothness of the fiber paths can be assured by applying a constraint on the minimum radius of curvature of the path. The tow angle distributions are controlled by the B-spline control points, which can be considered the inputs for the parameterization, and the outputs are the tow angle values at the nodes. For this work, we use shell elements whose stiffness matrices vary using the same shape functions as the displacements.

We use B-splines because of their many favorable properties—they have compact support, the number of control points and order can be arbitrarily controlled, and they have a constant Jacobian since they are linear with respect to the control point values. A B-spline surface is simply a tensor-product generalization of a B-spline curve and is mathematically defined as

$$P(u,v) = \sum_{i=1}^{m} \sum_{j=1}^{n} B_i(u) B_j(v) C_{ij},$$

where P is the output of the B-spline surface, C_{ij} are the control point values, u,v are the parametric coordinates, and B_k are the piecewise-polynomial basis functions. In this context, $P(u,v)$ would be the tow angle evaluated at a parametric location (u,v) in the structural component, which are assumed to be topologically 4-sided, and C_{ij} are the tow angle control points. Figure 2 shows the B-spline control point locations overlayed on a constant and a perturbed tow angle distribution.

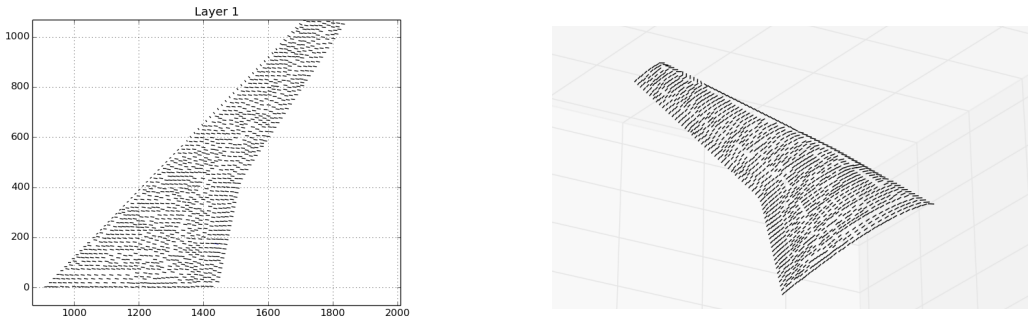

(a) 2D Parametric Map (b) 3D Curved Surface

Figure 3: Illustration of the local tow angle transformation.

4.2 Computation of the stiffness matrices
Given the tow angle at each node, the shell stiffness properties are calculated using FSDT; that is, we obtain the A, B, D, and A^* matrices. Prior to this, however, the nodal tow angles given by the B-spline parameterization must be transformed to obtain the equivalent angle in the elements frame that would produce the same effective angle. This transformation is pre-computed as an initialization step; starting with one of the elements, the algorithm marches out to neighboring elements, computing the rotation of each neighboring element relative to the current one. In each element, the pre-computed rotation is added to the tow angle from the global frame to obtain the correct angle in the local frame. This effectively guarantees a continuous fiber distribution so long as the surface can be transformed into the 2D mapping with at most one cut, so an example where this would not work would be a cube. This method can be generalized for any number of control points or laminae layers. A special case of this mapping is the case in which tow angle control points are all set to the same value, which in 3D corresponds to wrapping parallel lines around the curvature of the surface. The parametric warping process can be seen in Fig. 3.

4.3 Structural solver and optimizer
The structural solver used in this work is the toolkit for the analysis of composite structures (TACS) [7]. TACS is a general finite-element package that enables the implementation of custom elements and material models, but in this work, we use shell elements with a mixed interpolation of tensorial components (MITC) formulation and FSDT. TACS has been developed specifically for gradient-based optimization, so it provides the necessary routines to implement the adjoint method. The adjoint method enables the computation of a gradient at a cost roughly equal to running a single structural analysis, and this cost is independent of the number of design variables. For a detailed explanation of the adjoint method, the reader is referred to Martins and Hwang [10].

The optimizer we use in this work is SNOPT [2], an active-set reduced Hessian Sequential Quadratic Programming (SQP) algorithm. SNOPT is effective in solving large-scale nonlinear optimization problems with sparse constraints. We interface to SNOPT from Python via the pyOpt package [11]; pyOpt is an optimization suite that enables simple access to many optimizers with a common optimization problem definition.

5. Results

5.1 Optimization problem
Several compliance minimization problems will be considered, each of which takes the form .

$$\begin{aligned} \text{minimize} \quad & \tfrac{1}{2} u^T K u \\ \text{with respect to} \quad & \theta_{cp} \end{aligned}$$

The compliance is minimized subject to each of the control point tow angles parameterizing the design. For every case only a single ply optimization was considered, however multi-ply optimization is possible as well. The composite properties used for each problem are listed below in Tab. 1.

5.2. Verification of B-spline parameterization
To assess the robustness of the B-spline parameterization, we solved the optimization case originally proposed by Hvejsel et al. [1] . In this case, a 1 m x 1 m x 0.05 m plate is clamped on all edges and subjected to a uniform pressure loading on the top. The objective of this optimization is to minimize the compliance of the plate with

Table 1: Material Properties

Property	Value
E_1	54 GPa
E_2,E_3	18 GPa
G_{12}, G_{13}, G_{23}	9 GPa
ν_{12}	0.25

respect to the ply angles. In the case of Hvejsel et al. [1], the angles were forced to take discrete values. In our case, we relax that requirement and allow a continuous fiber distribution. The discrete case was used as a benchmark and the result can be seen in Fig. 4. The continuous optimization case was run with 25, 100, and 200 control points uniformly distributed throughout the plate, and in each case, we started with all the fibers in the x-direction. The optimization results are shown in Fig. 5. It can be seen that the optimal designs for the discrete and continuous cases are similar in pattern: the fibers point radially towards the edges and form a diamond toward the center. Due to their smooth nature the bi-splines have a more difficult time modeling the sharp angle changes seen in the boundary between the inner and outer square regions. The final compliance for the 25, 100, and 400 control point designs was 10.19 J, 9.18 J and 8.89 J, respectively. For reference, the discrete case yields a compliance of 8.83 J, while the initial zero degree case yields. It is not surprising to see that as the number of control point is increased, the minimum compliance decreases. While it is surprising that the continuous cases did not outperform the discrete case, it is important to note that due to the symmetry of the problem this case features local minima as is explored in the following section. Using different initial distributions, the solution will converge to a slightly better optimum.

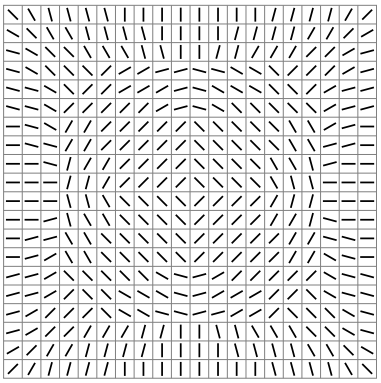

Figure 4: Solution to the discrete case (8.83 J).

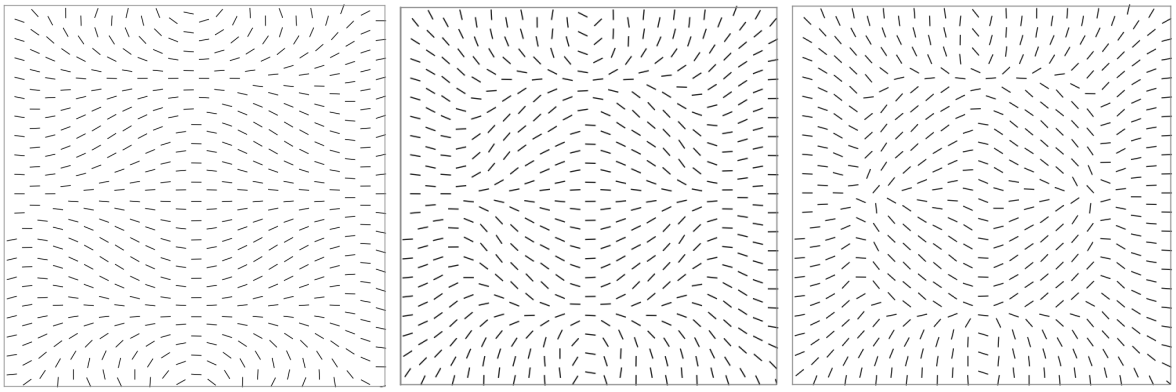

(a) 25 Control point case (10.19 J). (b) 100 Control point case (9.18 J). (c) 400 Control point case (8.89 J).

Figure 5: Clamped plate solutions for variable tow angles

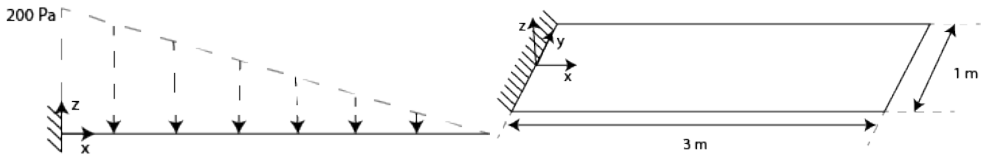

Figure 6: Cantilevered plate problem.

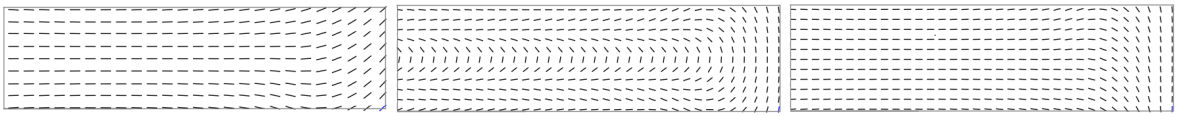

Case A: 45° Starting Point (8.45 J) Case B: 90° Starting Point (10.56 J) Case C: 92° Starting Point (8.45 J)

Figure 7: Cantilevered plate solutions.

5.2. Exploration of Local Minima

The next problem that was looked at was a simple cantilevered 3 m x 1 m x 0.01 m plate under a triangular distributed load shown in Fig. 6. The objective function was again compliance, which was minimized with respect to 40 control point ply angles. The global minimum to this problem is when all fibers point along the axis of bending, in this case the x-axis or 0° This problem was run with three different initial uniform tow distributions, of 45°, 90°, and 92°, corresponding to cases A, B, and C, respectively. The model contained 9801 elements with 60,000 degrees of freedom. The results for each case are shown in in Fig. 7. As was expected, in all three cases the optimizer tries to re-orientate the tow angles to 0°. The fibers furthest away from the clamped end change the least since the compliance is very insensitive to these values. What is interesting to note is that while case A and C converged to a compliance of 8.45 J case B only converged to 10.56 J, a difference of 25%. We can see from the pattern that while most of the fibers point along the x-axis there is a 'U' shaped pattern going down the center, preventing it from achieving the same value as cases A and C. The fact that the solution for case B and C differ so much despite only differing slightly in initial values seems to suggest that there is a local minimum to the problem due to the symmetry of the problem.

5.3. Structural Wing Box Optimization

The final problem that was considered was a full wing box modeled from the NASA Common Research Model (CRM). This wing box structure is created using GeoMACH [3], an open-source parametric modeler for aircraft geometries and structures. We first create the wing box geometry in GeoMACH, and once we specify the desired locations of the ribs, spars, and stringers, GeoMACH automatically generates a parametric unstructured quadrilateral mesh of the structure. In this work, we do not change the geometry of the wing.

For this problem the structure was loaded with a uniform suction pressure on the upper surface and an equal in magnitude positive pressure on the lower surface such that the net resultant force on the wing is upward. The magnitude of the pressure on both surfaces was 3.6 kPa. The model contains 16,659 elements with just under 100,000 degrees of freedom. The optimization was again a compliance minimization of the entire structure. The design variables consist of 80 tow angle control points, 40 on both the upper and lower skins of the wing box. This problem was run from two initial designs: one with the fibers pointing along the span of the wing and the other with the fibers pointed along the chord. The initial compliance was 28.7 MJ for the spanwise case, and 50.1 MJ for the chordwise case. Both cases converge to the solution seen in Fig8 (b) with a final compliance value of 25 MJ.This is a 50% and 13% improvement for the chordwise and spanwise cases respectively. The figures show the upper surface only, however the lower surface shares similar features in fiber distribution. While this is an impressive improvement for the chordwise distribution, clearly this case would represent one of the poorest engineering choices in practice. It is more informative to compare the optimum with the spanwise case, since this represents a more intuitive design choice. We can see that for the optimized wing, most of the fibers still point in the spanwise direction. The differences exist toward the trailing edge, where the fibers change direction sharply to point in the chordwise direction. The span-wise fibers on the main part of of the wing act to reduce the bending stresses, since this is where the load is carried. The reason for the sharp transition at the aft of the wing is that this juncture is where the ribs end the model, so the optimizer places the fibers in the chord-wise direction to make up for the loss of rigidity in the aft region.

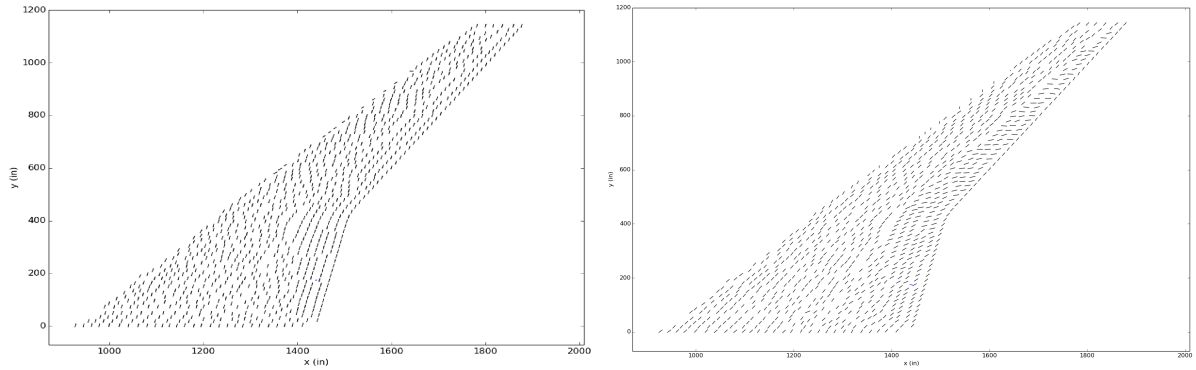

(a) Initial (b) Optimized

Figure 8: Initial and optimized tow angle distributions.

6. Conclusion

We presented a method for parameterizing and optimizing tow steered composite structures. We presented two 2D optimization problems to benchmark the performance of the parameterization, and included a third, more sophisticated, problem in three dimensions to demonstrate its utility. From our study we conclude that the method is indeed robust, however is limited in the sense that sharp tow angle changes are difficult to achieve. It has also been shown that certain problems may be subject to local minima due to the parameterization. While the optimization cases presented in this paper focused on compliance minimization it can be easily extended to more general optimization problems with multiple laminae layers.

7. Acknowledgments

The authors gratefully acknowledge support from NASA towards the provided in this paper.

8. References

[1] E. L. C. Hvejsel and M. Stolpe. Optimization strategies for discrete multi-material stiffness optimization. *Structural and Multidisciplinary Optimization*, (44):149–163, 2006.

[2] P. E. Gill, W. Murray, and M. A. Saunders. An SQP algorithm for large-scale constrained optimization. *Society for Industrial and Applied Mathematics*, 47(1), 2005.

[3] J. T. Hwang, G. K. W. Kenway, and J. R. R. A. Martins. Geometry and structural modeling for high-fidelity aircraft conceptual design optimization. In *Proceedings of the 15th AIAA/ISSMO Multidisciplinary Analysis and Optimization Conference*, Atlanta, GA, June 2014. AIAA 2014-2041.

[4] D. Jegley, B. Tatting, and Z. Gurdal. *Optimization of Elastically Tailored Tow-Placed Plates with Holes*. American Institute of Aeronautics and Astronautics, 2014/05/31 2003.

[5] C. V. Jutte, B. K. Stanford, C. D. Wieseman, and J. B. Moore. Aeroelastic tailoring of the nasa common research model via novel material and structural configurations. In *Proceedings of the AIAA 52nd Aerospace Sciences Meeting*, January 2014.

[6] G. J. Kennedy and J. R. R. A. Martins. A laminate parametrization technique for discrete ply angle problems with manufacturing constraints. *Structural and Multidisciplinary Optimization*, 48(2):379–393, August 2013.

[7] G. J. Kennedy and J. R. R. A. Martins. A parallel finite-element framework for large-scale gradient-based design optimization of high-performance structures. *Finite Elements in Analysis and Design*, 87:56–73, September 2014.

[8] G. K. W. Kenway and J. R. R. A. Martins. Multipoint high-fidelity aerostructural optimization of a transport aircraft configuration. *Journal of Aircraft*, 51(1):144–160, January 2014.

[9] A. B. Lambe and J. R. R. A. Martins. Extensions to the design structure matrix for the description of multidisciplinary design, analysis, and optimization processes. *Structural and Multidisciplinary Optimization*, 46:273–284, August 2012.

[10] J. R. R. A. Martins and J. T. Hwang. Review and unification of methods for computing derivatives of multidisciplinary computational models. *AIAA Journal*, 51(11):2582–2599, November 2013.

[11] R. E. Perez, P. W. Jansen, and J. R. R. A. Martins. pyOpt: a Python-based object-oriented framework for nonlinear constrained optimization. *Structural and Multidisciplinary Optimization*, 45(1):101–118, January 2012.